Distinctive facial features in Andersen-Tawil syndrome: a three-dimensional stereophotogrammetric analysis

Claudia Dolci[1*], Valeria A. Sansone[2*], Daniele Gibelli[1], Annalisa Cappella[1], Chiarella Sforza[1]

* Claudia Dolci and Valeria A. Sansone should be considered joint first author

1. Functional Anatomy Research Center (FARC), Laboratorio di Anatomia Funzionale dell'Apparato Stomatognatico (LAFAS), Department of Biomedical Sciences for Health Università degli Studi di Milano, Milan, Italy
2. NEuroMuscularOmnicenter, NEMO Clinical Center, Neurorehabilitation Unit, Università degli Studi di Milano, Milan, Italy

MS submitted to *American Journal of Medical Genetics Part A* on 1 September 2020
Revised: 19 Novembre 2020; Accepted: 14 December 2020

Running title: 3D facial morphometry in Andersen-Tawil syndrome

Presented in abstract form at the 73rd National Congress of the Italian Society of Anatomy and Histology (Napoli – Italy, 2019)

Number of tables: 2

Number of figures: 4

Corresponding author:
Dr. Claudia Dolci
Department of Biomedical Sciences for Health
Università degli Studi di Milano
Via Mangiagalli 31
20133 Milan - Italy
Phone: +39 02 503 15392; Fax: +39 02 503 15387
claudia.dolci@unimi.it

This is the accepted version of the following article:
Dolci C, Sansone VA, Gibelli D, Cappella A, Sforza C. Distinctive facial features in Andersen-Tawil syndrome: A three-dimensional stereophotogrammetric analysis. Am J Med Genet A. 2021 Mar;185(3):781-78. DOI: 10.1002/ajmg.a.62040

Distinctive facial features in Andersen-Tawil syndrome: a three-dimensional stereophotogrammetric analysis

ABSTRACT

Andersen-Tawil syndrome (ATS) is a rare potassium channelopathy causing periodic paralysis, cardiac arrhythmias, and dysmorphic features. A detailed analysis of the face could facilitate diagnosis of ATS, as approximately 30% of patients do not show variants in *KCNJ2* gene, and diagnosis is established by clinical findings. We aimed to characterize the face in ATS through a quantitative approach, as facial anomalies may be unnoticed on visual inspection. Facial images of 12 subjects with genetically confirmed ATS (6 males, 6 females, age 5-67 years) were acquired through stereophotogrammetry. Using 38 soft-tissue landmarks, linear distances, angles, and ratios were calculated and expressed as z-score values, with reference to 477 healthy subjects matched for sex and age. All patients showed decreased lower facial height with shortening of philtrum (mean z-score±SD: -1.5±0.9), smaller mid and lower facial depths (-1.9±0.7; -2.3±0.9), short palpebral fissures (right -1.2±0.4; left -1.6±0.6), smaller mandibular ramus length (-2.1±0.4), and increased nasal width/length ratio (1.4±0.5) with smaller nostril axis length (right -1.8±0.8, left -1.6±0.7). Hypertelorism and low-set ears were detected in two-thirds of patients. The study quantified facial dysmorphysm in ATS, extending information about known features, and detecting unrecorded philtrum and nostril characteristics which may be distinctive traits of the disorder.

Key words: Andersen-Tawil syndrome; facial feature, 3D; stereophotogrammetry; anthropometry.

INTRODUCTION

Andersen-Tawil syndrome (ATS, OMIM #170390) is a hereditable autosomic dominant channelopathy with prevalence estimated at about 1:500,000 (Maffè et al., 2020). The disorder is associated with mutations in the *KCNJ2* gene on chromosome 17 (ATS type 1), which encodes for Kir2.1, an inward rectifier potassium channel involved in stabilizing resting membrane potential and modulating the repolarization phase in excitable cells (Plaster et al., 2001); recently, also *KCNJ5* gene encoding for Kir3.4 potassium channel has been associated with the disorder (ATS type 2) (Kokunai et al., 2014).

Skeletal and cardiac muscles are affected, resulting in episodes of muscle weakness especially following prolonged rest or rest after exertion, and cardiac dysrhythmias. Dysmorphic features also characterize the disorder (Sansone, & Tawil, 2007). Short stature, fifth-digit clinodactyly and syndactyly of toes two and three are the most typical skeletal characteristics of the disease, which is also associated with distinctive facial features and poor dentition. Common facial characteristics include small mandible, low-set ears, and widely spaced eyes; however the spectrum of anomalies is wider and includes broad forehead, short palpebral fissures, malar and maxillary hypoplasia, nose with broad base, bulbous tip or fullness alongside the bridge, thin upper lip, triangular face, and mild facial asymmetry (Davies et al., 2005; Yoon et al., 2006).

In about 60-70% of cases, ATS is caused by a mutation in the causative gene (Nguyen, Pieper, & Wilders, 2013); the exact manner this mutation induces an altered development of the face is a matter of great interest (Adams et al., 2016; Belus et al., 2018). In the remaining third of cases, the underlying genetic mutation is still unknown: since patients show the same phenotypic features, diagnosis is established by clinical findings.

ATS can manifest with the typical symptomatic triad, namely periodic paralysis, ventricular arrhythmias and dysmorphic features, thus suggesting the diagnosis. However, patients may

distinctly exhibit only one or none of them: the great phenotypic variability, even intrafamilial, and the rarity of the disease may lead to a challenging diagnosis (Ardissone, Sansone, Colleoni, Bernasconi, & Moroni, 2017). On the other hand, because some of the cardiac manifestations of ATS can be dangerous and predispose to cardiac arrest (Peters, Schulze-Bahr, Etheridge, & Tristani-Firouzi, 2007; Airey, Etheridge, Tawil, & Tristani-Firouzi, 2009; Maffè et al., 2020), establishing an early and accurate diagnosis of the disorder is essential to start appropriate treatment and follow-up. The recognition of distinctive facial features can help early diagnosis of ATS, but manifestations may be subtle and therefore unnoticeable on routine physical examination (Canun, Perez, & Beirana, 1999; Tristani-Firouzi, & Etheridge, 2010). Except for a few anthropometric measurements (Yoon et al., 2006), a quantitative definition of facial dysmorphism associated with ATS is not available, and clinicians routinely evaluate them through subjective visual inspection.

Today, a detailed and reliable analysis of facial structures can be performed using three-dimensional (3D) image acquisition systems (Sforza, de Menezes, & Ferrario, 2013); an accurate 3D morphometric assessment of the face can allow to detect even subtle but specific features, thus helping to improve the diagnosis of a disorder associated with facial dysmorphism (Pucciarelli et al., 2017; Dolci et al., 2018; Ji et al., 2020). Among safe and noninvasive optical devices, stereophotogrammetry is fast and simple to use, thus being suitable for the quantitative evaluation of facial dysmorphisms even in uncooperative subjects like young children or people with special needs (Pucciarelli et al., 2019; Gibelli, Dolci, Cappella, & Sforza, 2020; Masnada et al, 2020).

The study aimed to better define the facial phenotype associated with ATS through stereophotogrammetry, in order to facilitate the early diagnosis of the disease.

METHODS

Participants and 3D facial acquisition

Twelve subjects with *KCNJ2* gene mutation confirmed diagnosis of ATS were recruited for the study. They were aged 5-67 years: 6 males (mean ± SD 34 ± 28 years) and 6 females (mean ± SD age: 33 ± 11 years) from 6 Italian unrelated families, except for 2 patients whose father was of North African origin. One patient had a previous history of corrective surgery for cleft palate. Males were asked to remove mustache or beard. Furthermore, 477 Italian healthy subjects (314 males and 163 females), matched with patients for sex and age, were evaluated to serve as reference group. All participants, and their parents if they were minors, in accordance with the Declaration of Helsinki gave written consent to the study procedure, which was preventively approved by the ethics committee of the University of Milan (26.03.14, n° 92/14).

For each subject, facial anthropometric data collection was carried out in successive steps. At first, an expert operator identified 38 facial soft-tissue anatomical landmarks (8 midline and 15 paired) through visual inspection or palpation, marking them on the skin with a common eyeliner. Landmarks were chosen according to international criteria (Farkas, 1994), and to a protocol developed by our laboratory to describe the face *in toto* and its different portions (facial thirds, orbital region, nose, ears, lips) (Ferrario, Sforza, Serrao, Ciusa, & Dellavia, 2003; Tartaglia, Dolci, Sidequersky, Ferrario, & Sforza, 2012), and quantify dysmorphisms also associated to genetic and neuromuscular disorders (Dolci et al., 2018; Pucciarelli et al., 2019). Subsequently, subjects underwent facial photographs through stereophotogrammety (VECTRA M3, Canfield Scientific, Fairfield, NJ, USA), while sitting with a natural head position and neutral facial expression. The instrument consists of 2 cameras for each of 3 appropriately arranged modules that image the face simultaneously from different points of view, thus allowing a detailed 3D reconstruction of the facial image (capture time: 3.5 ms;

geometric resolution: 1.2 mm). After the subjects left the laboratory, the landmark digitization was performed off line on each 3D facial image and their x, y, z, coordinates were extracted for subsequent data elaboration. Repeatability and accuracy of data collection procedure were verified (de Menezes, Rosati, Ferrario, & Sforza, 2010). Figure 1 shows an example of 3D reconstruction of the face of a subject with ATS and the landmarks used in the study. From the landmark coordinates, 28 facial linear distances, 3 ratios, and 13 angles in all three spatial directions were automatically calculated by a custom computer program (Tables 1 and 2). Furthermore, the presence of low-set ears was evaluated and quantified in patients with ATS, verifying if the insertion of the helix to the scalp was positioned below a horizontal plane passing through both inner canthi of the eyes (Hunter et al., 2009).

Statistical analysis

Individual raw values were converted to z-scores (number of standard deviations below or above the mean value of appropriate reference group) to control for sex and age differences: the smaller the z-score in absolute value, the closer the patient value to the healthy subject one. Mean z-scores were compared with those of the healthy subjects using a paired Student's t test (level of significance set at 1%), after checking for normal distribution of individual values. They were first calculated separately for males and females. Since respective values did not show any statistically significant difference (Mann–Whitney U test, $p > 0.05$), they were pooled.

RESULTS

Several facial anthropometric measurements showed significant differences when comparing patients with ATS to healthy subjects (Tables 1 and 2, z-score values; Fig. 2, percentage variations).

Patients showed an overall mild but significant smaller facial height, mainly due to a reduction of its lower part (Fig. 3A). Noteworthy, a significant decrease of nasolabial philtrum length was observed within this portion of the face (negative z-scores in 12/12 subjects; z-score < -2 in 6/12 subjects from 4 families). Significant differences concerning vermillion characteristics were not found, even if two-third of patients showed negative z-score values for upper vermillion height (z-score values < -2 in 3/12 subjects). Since patients showed a slight decrease in facial width, the facial width/height ratio was significantly even not remarkably increased. On the whole, patients did not show increased height of forehead, being 0.4 the only individual positive z-score value.

Patients with ATS showed a slight but significant greater facial divergence and reduced facial height index (FHI) (Fig. 3B), being the two measurements influenced by a remarkable shorter mandibular ramus (negative z-score value in all subjects; z-score value $\leq$ 2 in 8/12) in addition to the decreased smaller lower facial height. All other mandibular anthropometric measurements (body length, width, convexity, and mandibular angles) did not show any significant differences between patients and healthy subjects.

Patients showed smaller facial depths (Fig. 3C), with a progressive remarkable reduction of values from the upper to the lower part of the face (negative z-score value in all subjects); consistently, the corresponding facial convexities in the horizontal plane showed a gradual increase from the forehead (t-n-t angle) to the midfacial (t-prn-t) and chin regions (t-pg-t angle). Facial convexities in the sagittal plane were similar in patients and reference groups.

Concerning the orbital region, patients showed significant smaller intercanthal (or palpebral fissure) length (negative z-score value in all subjects, with asymmetry between the two sides in 10/12); an increase of inner canthal width was detected in two-thirds of patients, even if only 4 of them had z-score values ≥ 1). The inclinations of the right and left palpebral fissure versus the true horizontal were slightly but significantly decreased (z-score value < -1 in 9/12 patients), thus producing a tendency to palpebral downslanting. The height of the orbit and its inclination versus the true horizontal were not significantly different in patients and healthy subjects.

Pointing at nose anthropometric features, patients showed a slight but significant increase of nose width (positive z-score value in all subjects; z-score value > 2 in 3/12); together with the slight but significant reduced nose length (or upper facial height), the finding influenced a significant increase of nasal width/length ratio. On both sides, patients showed a smaller length of nostril axis (z-score value < -1 in 11/12 subjects) with asymmetry between sides to some extent, and a slight but significant larger interalar angle (positive z-score value in 11/12 subjects) (Fig. 4).

Widely spaced eyes were detected in two-thirds of patients. Ears were not different in patients and healthy subjects, both for height and width, but low set-ears were detected in two-thirds of patients; the insertion of helix on the scalp below the horizontal plane passing through the inner canthi of the eyes ranged from 0.5 to 2.5 cm, being symmetric for the two ears in all patients.

DISCUSSION

Human face development is a very complex multifactorial process and it is not surprising that at least 30-40% of the hereditable human disorders display some manifestations relating to the craniofacial district, including ATS (Hart, & Hart, 2009). They are not always easily detectable on clinical inspection but the lack of their recognition can lead to an undesirable delay in diagnosis. Since reliable anthropometric measurements assure objectivity in dysmorphology (Dalal, & Phadke, 2007), and craniofacial anomalies are one of the three criteria used for diagnosis of ATS, we analyzed the facial phenotype associated with ATS performing a detailed 3D morphometric evaluation of the face.

Among the modern safe techniques for the 3D reconstruction of the facial surface, stereophotogrammetry overcame several limits of direct anthropometry, such as the risk of motion artifacts, being very fast in capturing a facial image, and the risk of soft-tissue deformations, because it does not need any contact between the instrument and the skin. Also due to the large amount of collectible data concerning a face, stereophotogrammetry is considered the gold standard for facial scans; it is increasingly used both for research and clinical purposes in a variety of disciplines interested in a detailed analysis of the face and its parts, including genetics, maxillofacial, reconstructive and aesthetic surgery, and forensic medical sciences (Gibelli, Dolci, Cappella & Sforza, 2020; Ji et al., 2020). The limitations on the use of the device, mainly concerning with considerable costs and the need for an appropriate size of acquisition setting, can be partially overcome by smaller portable instruments, which have proved to be accurate enough for most clinical applications (Gibelli, Dolci, Cappella, & Sforza, 2020).

Facial morphometric features analyzed in this study were measured following the manual digitization of anthropometric landmarks on each 3D facial image. It has to be mentioned that

novel promising methods for automatic localization of landmarks on 3D faces could be useful to save time and reduce the need for experienced operators (Marcolin, & Vezzetti, 2017).

We analyzed facial features pooling male and female data, after verifying they were not different. Krych et al. (2017) reported that few studies analyzed data concerning ATS manifestations in both sexes, with contrasting results in relation to cardiac and skeletal muscle phenotypes; Andelfinger et al. (2002) did not find sex specificity for dysmorphic features.

In the current study, all patients showed negative z-score values for both the height and depth of the lower third of the face, thus confirming small mandible as distinctive facial feature of ATS. Our finding concord with the study by Yoon et al. (2006), who observed mandibular hypoplasia in all 10 examined subjects through anthropometric evaluation. Differently, in studies on KCNJ2 mutation carriers by Tristani-Firouzi et al. (2002) and Krych et al. (2017), a small mandible was observed in 16/36 (44%) and 15/25 (60%) patients respectively. Phenotypic variability in ATS is well known and may explain that discrepancy; nevertheless, a quantitative evaluation of facial structures can detect small variations which might not be noticed on a mere visual inspection of patients. Also the depth, and to some extend the height of the middle third of the face, were reduced in all patients, in accordance with maxillary hypoplasia observed by Yoon et al. (2006). More than 20 years ago it has been demonstrated the *KCNJ2* gene expression in bone-associated developing structures of the rat head, as well as limb and body, thus opening the way for understanding the etiology of craniofacial anomalies in ATS (Karschin, & Karschin, 1997). Nowadays it is known that normal Kir2.1 potassium channel activity is required for the correct development of craniofacial structures (Adams et al., 2016). Interestingly, KCNJ2 knock-out mice embryos show an abnormal development of structures derived from cranial neural crest, including hypoplastic mandible, maxilla, premaxilla and prenasal bones (Belus et al., 2018). None of the patients showed an increased height of the forehead. It can be hypothesized that the broad forehead frequently

reported for subjects with ATS is to be considered relative to the small face of the patients or it is only the result of its widening.

When compared to the healthy reference group, patients with ATS showed increased facial divergence and decreased facial height index (FHI). In all patients both the measurements were influenced by a remarkable decrease of the mandibular ramus length; also considering that mandibular angles did not vary significantly from reference subjects, that finding is consistent with low-set ears. Actually, we detected that feature in two-thirds of patients.

As regards the orbital region, all patients showed a decrease in palpebral fissure length, thus confirming a known characteristic for the syndrome, even if it is not included among the three facial supportive diagnostic criteria (Statland et al., 2018). Almost all patients showed differences between the two sides, being the left palpebral fissure shorter than the right one. The finding is in accordance with the mild facial asymmetry observed in patients with ATS by Yoon et al. (2006). Two-third of the patients showed slight palpebral fissure downslanting. Actually, that feature is rarely reported in literature (Sacconi et al., 2009), and it might be considered a familiar trait. On the whole, patients did not show a significant increase of inner canthal width; indeed two-thirds of them showed positive z-score values, but mostly being smaller than 1. Frequencies of hypertelorism differ greatly among studies, being reported in 8/10 (80%) patients by Yoon et al. (2006), and 4/41 (10%) of patients with a specific mutation in *KCNJ2* gene by Andelfinger et al. (2002). Beyond possible differences due to the method of evaluation (inner canthal width versus interpupillary distance), discrepancies may be explained by the phenotypic variability of ATS, or the facial phenotype could be influenced by the type of *KCNJ2* mutation; nevertheless, it cannot be excluded that on visual inspection the distance between eyes could be overestimated, being the evaluation influenced by short palpebral fissures.

Morphometric analysis of the face in ATS patients pointed out a feature never described before: half of the patients had a clearly shortened nasolabial philtrum, the other half showing at least a decrease in its length. Actually, a thin upper lip is included among the distinctive facial features of the syndrome; however, it only refers to the vermillion, that was distinctly reduced also in one third of our patients. Nasolabial philtrum shows distinctive features in several syndromes associated with congenital facial dysmorphisms: the reduced nasolabial philtrum length detected in all our patients is consistent with a hypoplastic maxilla and could be a typical manifestation of ATS.

Patients showed an increased width of the nose, thus confirming a known phenotypic facial feature of the syndrome. The slight increase of interalar angle suggests also a tendency to a lesser protruding nose; however, on visual inspection that feature might be masked by the coexistence of a bulbous tip associated with the syndrome (Yoon et al., 2006). No studies reported any abnormal features in nostrils of patients with ATS. In the current study patients did not show peculiar nostril forms, not even heart-shape nostrils which are observed in wider noses more frequently (Etöz, Etöz, & Ercan, 2008). Conversely, almost all our patients showed a clear decrease in nostrils axis length, suggesting it might be helpful to include their examination when evaluating the face of a patients suspected for ATS.

The small number of the recruited patients because of the rarity of the syndrome is the major limitation in this study: a multicenter study with a larger cohort would allow to strengthen the findings. Additionally, our patients were enrolled in the study independently from their specific mutation in *KCNJ2* gene; facial phenotype differences could better emerge when evaluating homogeneous groups of patients.

In conclusion, the study allowed to enhance knowledge concerning the facial phenotype in ATS, and first identified anthropometric facial features which could be distinctive traits of the disorder. 3D quantitative assessment of facial morphology allowed the detection of even very

subtle facial abnormalities which could elude a clinical examination based only on a subjective inspection of the patients. An accurate 3D morphometric analysis of the face could help in improving early recognition of ATS, particularly when the distinctive facial features are not clearly manifest, in order to start an effective management and follow up of the disease. This is especially important because recent longitudinal data on cardiac involvement provide evidence that the clinical course of patients with ATS type 1 is characterized by a high rate of life-threatening adverse events (Mazzanti et al., 2020).

ACKNOWLEDGEMENTS

The authors are grateful to all the subjects who volunteered for the study.

CONFLICT OF INTEREST STATEMENT

The authors have no conflicts of interest related to the current investigation.

FINANCIAL SUPPORT

Financial support was obtained from University of Milan (Piano di sostegno alla ricerca 2017-2019).

ETHICS

The investigation complies with the principles stated in the Declaration of Helsinki "Ethical Principles for Medical Research Involving 'Human Subjects". Ethical approval obtained by the ethical committee of Università degli Studi di Milano, Milan, Italy (26.03.14; n° 92/14).

AUTHOR CONTRIBUTIONS

Claudia Dolci: study design, data collection, analysis and interpretation, drafting the paper, final approval of the submission.

Valeria Sansone: study design, data interpretation, drafting the paper, final approval of the submission.

Daniele Gibelli: data collection and interpretation, revising the papers' draft for important intellectual concepts, final approval of the submission.

Annalisa Cappella: data collection and interpretation, revising the papers' draft for important intellectual concepts, final approval of the submission.

Chiarella Sforza: study design, data analysis and interpretation, revising the papers' draft for important intellectual concepts, final approval of the submission.

DATA AVAILABILITY STATEMENT

The data that support the findings of this study are available on request from the corresponding author. The data are not publicly available due to privacy and ethical restrictions.

REFERENCES

Adams, D.S., Uzel, S.G., Akagi, J., Wlodkowic, D., Andreeva, V., Yelick, P.C., Devitt-Lee, A., Pare, J.F., & Levin, M. (2016). Bioelectric signalling via potassium channels: a mechanism for craniofacial dysmorphogenesis in KCNJ2-associated Andersen-Tawil Syndrome. *The Journal of Physiology*, 594, 3245-3270. https://doi.org/10.1113/JP271930

Airey, K.J., Etheridge, S.P., Tawil, R., & Tristani-Firouzi, M. (2009). Resuscitated sudden cardiac death in Andersen-Tawil syndrome. *Heart Rhythm*, 6, 1814-1817. https//doi.org/ 10.1016/j.hrthm.2009.08.032

Andelfinger, G., Tapper, A.R., Welch, R.C., Vanoye, C.G., George, A.L. Jr, & Benson, D.W. (2002). KCNJ2 mutation results in Andersen syndrome with sex-specific cardiac and skeletal muscle phenotypes. *The American Journal of Human Genetics*, 71, 663-668. https://doi.org/10.1086/342360

Ardissone, A., Sansone, V., Colleoni, L., Bernasconi, P., & Moroni, I. (2017). Intrafamilial phenotypic variability in Andersen-Tawil syndrome: a diagnostic challenge in a potentially treatable condition. *Neuromuscular Disorders*, 27, 294-297. https://doi.org/10.1016/j.nmd.2016.11.006

Belus, M.T., Rogers, M.A., Elzubeir, A., Josey, M., Rose, S., Andreeva, V., Yelick, P.C., & Bates, E.A. (2018). Kir2.1 is important for efficient BMP signaling in mammalian face development. *Developmental Biology*, 444, S297-S307. https://doi.org/10.1016/j.ydbio.2018.02.012

Canun, S., Perez, N., & Beirana, L.G. (1999). Andersen syndrome autosomal dominant in three generations. *American Journal of Medical Genetics*, 85, 147-156. https://doi.org/10.1002/(sici)1096-8628(19990716)85:2<147::aid-ajmg9>3.0.co;2-0

Dalal, A.B., & Phadke, S.R. (2007). Morphometric analysis of face in dysmorphology. *Computer Methods and Programs in Biomedicine*, 85, 165-172. https://doi.org/10.1016/j.cmpb.2006.10.005

Davies, N.P., Imbrici, P., Fialho, D., Herd, C., Bilsland, L.G., Weber, A., Mueller, R., Hilton-Jones, D., Ealing, J., Boothman, B.R., Giunti, P., Parsons, L.M., Thomas, M., Manzur, A.Y., Jurkat-Rott, K., Lehmann-Horn, F., Chinnery, P.F., Rose, M., Kullmann, D.M., & Hanna, M.G. (2005). Andersen-Tawil syndrome: new potassium channel mutations and possible phenotypic variation. *Neurology*, 65, 1083-1089. https://doi.org/10.1212/01.wnl.0000178888.03767.74

De Menezes, M., Rosati, R., Ferrario, V.F., & Sforza, C. (2010). Accuracy and reproducibility of a 3-dimensional stereophotogrammetric imaging system. *Journal of Oral and Maxillofacial Surgery*, 68, 2129-2135. https://doi.org/10.1016/j.joms.2009.09.036

Dolci, C., Pucciarelli, V., Gibelli, D.M., Codari, M., Marelli, S., Trifirò, G., Pini, A.,& Sforza, C. (2018). The face in Marfan syndrome: a 3D quantitative approach for a better definition of dysmorphic features. *Clinical Anatomy*, 31, 380-386. https://doi.org/10.1002/ca.23034

Etöz, B.C., Etöz, A., & Ercan, I. (2008). Nasal shapes and related differences in nostril forms: a morphometric analysis in young adults. *Journal of Craniofacial Surgery*, 19, 1402-1408. https://doi.org/10.1097/SCS.0b013e31818530a7

Farkas, L.G. (1994). *Anthropometry of the head and face* (2nd ed.) New York, NY: Raven Press.

Ferrario, V.F., Sforza, C., Serrao, G., Ciusa, V., & Dellavia, C. (2003). Growth and aging of facial soft tissues: a computerized three-dimensional mesh diagram analysis. *Clinical Anatomy*, 16, 420-433. https://doi.org/10.1002/ca.10154

Gibelli, D., Dolci, C., Cappella, A., & Sforza, C. (2020). Reliability of optical devices for three-dimensional facial anatomy description: a systematic review and meta-analysis. *International Journal of Oral and Maxillofacial Surgery*, 49, 1092-1106. https://doi.org/10.1016/j.ijom.2019.10.019

Hart, T.C., & Hart, P.S. (2009). Genetic studies of craniofacial anomalies: clinical implications and applications. *Orthodontics & Craniofacial Research*, 12, 212-220. https://doi.org/10.1111/j.1601-6343.2009.01455.x

Hunter, A., Frias, J., Gillessen-Kaesbach, G., Hughes, H., Jones, K., & Wilson, L. (2009). Elements of morphology: Standard terminology for the ear. *American Journal of Medical Genetics Part A*, 149, 40–60. https:/doi.org/10.1002/ajmg.a.32599

Ji, C., Yao, D., Li, M.Y., Chen, W.J., Lin, S.L., & Zhao, Z.Y. (2020). A study on facial features of children with Williams syndrome in China based on three-dimensional anthropometric measurement technology. *American Journal of Medical Genetics Part A,* 182, 2102-2109. https://doi.org/10.1002/ajmg.a.61750

Karschin, C., & Karschin, A. (1997). Ontogeny of gene expression of Kir channel subunits in the rat. *Molecular and Cellular Neuroscience*, 10, 131-148. https://doi.org/10.1006/mcne.1997.0655

Kokunai, Y., Nakata, T., Furuta, M., Sakata, S., Kimura, H., Aiba, T., Yoshinaga, M., Osaki, Y., Nakamori, M., Itoh, H., Sato, T., Kubota, T., Kadota, K., Shindo, K., Mochizuki, H., Shimizu, W., Horie, M., Okamura, Y., Ohno, K., & Takahashi, M.P. (2014). A Kir3.4 mutation causes Andersen-Tawil syndrome by an inhibitory effect on Kir2.1. *Neurology*, 82, 1058-1064. https://doi.org/10.1212/WNL.0000000000000239

Krych, M., Biernacka, E.K., Ponińska, J., Kukla, P., Filipecki, A., Gajda, R., Hasdemir, C., Antzelevitch, C., Kosiec, A., Szperl, M., Płoski, R., Trusz-Gluza, M., Mizia-Stec, K., & Hoffman, P. (2017). Andersen-Tawil syndrome: clinical presentation and predictors of symptomatic arrhythmias - Possible role of polymorphisms K897T in KCNH2 and H558R in SCN5A gene. *Journal of Cardiology*, 70, 504-510. https://doi.org/10.1016/j.jjcc.2017.01.009

Maffè, S., Paffoni, P., Bergamasco, L., Dellavesa, P., Zenone, F., Baduena, L., Franchetti Pardo, N., Careri, G., Facchini, E., Sansone, V., & Parravicini, U. (2020). Therapeutic management of ventricular arrhythmias in Andersen-Tawil syndrome. *Journal of Electrocardiology*, 58, 37-42. https://doi.org/10.1016/j.jelectrocard.2019.10.009

Marcolin, F., & Vezzetti, E. (2017). Novel descriptors for geometrical 3D face analysis. *Multimedia Tools and Applications*, 76, 13805-13834. https://doi.org/10.1007/s11042-016-3741-3

Masnada, S., Gibelli, D., Dolci, C., De Giorgis, V., Cappella, A., Veggiotti, P., & Sforza, C. (2020). 3D facial morphometry in Italian patients affected by Aicardi syndrome. *American Journal of Medical Genetics Part A*, 182, 2325-2332. https://doi.org/10.1002/ajmg.a.61791

Mazzanti, A., Guz, D., Trancuccio, A., Pagan, E., Kukavica, D., Chargeishvili, T., Olivetti, N., Biernacka, E.K., Sacilotto, L., Sarquella-Brugada, G., Campuzano, O., Nof, E., Anastasakis, A., Sansone, V.A., Jimenez-Jaimez, J., Cruz, F., Sánchez-Quiñones, J., Hernandez-Afonso, J., Fuentes, M.E., Średniawa, B., Garoufi, A., Andršová, I., Izquierdo, M., Marinov, R., Danon, A., Expósito-García, V., Garcia-Fernandez, A., Muñoz-Esparza, C., Ortíz, M., Zienciuk-Krajka, A., Tavazzani, E., Monteforte, N., Bloise, R., Marino, M., Memmi, M., Napolitano, C., Zorio, E., Monserrat, L., Bagnardi, V., & Priori, S.G. (2020). Natural History and Risk Stratification in Andersen-Tawil Syndrome Type 1. *Journal of the American College of Cardiology*, 75, 1772-1784. https://doi.org/10.1016/j.jacc.2020.02.033

Nguyen, H.L., Pieper, G.H., & Wilders, R. (2013). Andersen-Tawil syndrome: clinical and molecular aspects. *International Journal of Cardiology*, 5, 1-16. https://doi.org/10.1016/j.ijcard.2013.10.010

Peters, S., Schulze-Bahr, E., Etheridge, S.P., & Tristani-Firouzi, M. (2007). Sudden cardiac death in Andersen-Tawil syndrome. *Europace*, 9, 162-166. https://doi.org/10.1093/europace/eul188

Plaster, N.M., Tawil, R., Tristani-Firouzi, M., Canún, S., Bendahhou, S., Tsunoda, A., Donaldson, M.R., Iannaccone, S.T., Brunt, E., Barohn, R., Clark, J., Deymeer, F., George, A.L. Jr, Fish, F.A., Hahn, A., Nitu, A., Ozdemir, C., Serdaroglu, P., Subramony, S.H., Wolfe, G., Fu, Y.H., & Ptácek, L.J. (2001). Mutations in Kir2.1 cause the developmental and episodic electrical phenotypes of Andersen's syndrome. *Cell*, 105, 511-519. https://doi.org/10.1016/s0092-8674(01)00342-7

Pucciarelli, V., Bertoli, S., Codari, M., De Amicis, R., De Giorgis, V., Battezzati, A., Veggiotti, P., & Sforza, C. (2017). The face of Glut1-DS patients: A 3D craniofacial morphometric analysis. *Clinical Anatomy*, 30, 644-652. https://doi.org/10.1002/ca.22890

Pucciarelli, V., Gibelli, D., Mastella, C., Bertoli, S., Alberti, K., De Amicis, R., Codari, M., Dolci, C., Battezzati, A., Baranello, G., & Sforza, C. (2020). 3D Facial morphology in children affected by spinal muscular atrophy type 2 (SMAII). *European Journal of Orthodontics*, 42, 500-508. https://doi.org/10.1093/ejo/cjz071

Sacconi, S., Simkin, D., Arrighi, N., Chapon, F., Larroque, M.M., Vicart, S., Sternberg, D., Fontaine, B., Barhanin, J., Desnuelle, C., & Bendahhou, S. (2009). Mechanisms underlying Andersen's syndrome pathology in skeletal muscle are revealed in human myotubes. *American Journal of Physiology-Cell Physiology*, 297, C876-C885. https://doi.org/10.1152/ajpcell.00519.2008

Sansone, V., & Tawil, R. (2007). Management and treatment of Andersen-Tawil syndrome (ATS). *Neurotherapeutics*, 4, 233-237. https://doi.org/10.1016/j.nurt.2007.01.005

Sforza, C., de Menezes, M., & Ferrario, V. (2013). Soft- and hard-tissue facial anthropometry in three dimensions: what's new. *Journal of Anthropological Sciences*, 91, 159-184. https://doi.org/10.4436/jass.91007

Statland, J.M., Fontaine, B., Hanna, M.G., Johnson, N.E., Kissel, J.T., Sansone, V.A., Shieh, P.B., Tawil, R.N., Trivedi, J., Cannon, S.C., & Griggs, R.C. (2018). Review of the diagnosis and treatment of periodic paralysis. Muscle & Nerve, 57, 522-530. https://doi.org/10.1002/mus.26009

Tartaglia, G.M., Dolci, C., Sidequersky, F.V., Ferrario, V.F., & Sforza, C. (2012). Soft tissue facial morphometry before and after total oral rehabilitation with implant-supported prostheses. *Journal of Craniofacial Surgery*, 23, 1610-1614. https://doi.org/10.1097/SCS.0b013e31825af109

Tristani-Firouzi, M., Jensen, J.L., Donaldson, M.R., Sansone, V., Meola, G., Hahn, A., Bendahhou, S., Kwiecinski, H., Fidzianska, A., Plaster, N., Fu, Y.H., Ptacek, L.J., & Tawil,

R. (2002). Functional and clinical characterization of KCNJ2 mutations associated with LQT7 (Andersen syndrome). *The Journal of Clinical Investigation*, 110, 381-388. https://doi.org/10.1172/JCI15183

Tristani-Firouzi, M., & Etheridge, S.P. (2010). Kir 2.1 channelopathies: the Andersen-Tawil syndrome. *Pflügers Archiv European Journal of Physiology*, 460, 289-294. https://doi.org/10.1007/s00424-010-0820-6

Yoon, G., Oberoi, S., Tristani-Firouzi, M., Etheridge, S.P., Quitania, L., Kramer, J.H., Miller, B.L., Fu, Y.H., & Ptácek, L.J. (2006). Andersen-Tawil syndrome: prospective cohort analysis and expansion of the phenotype. *American Journal of Medical Genetics Part A*, 140, 312-321. https://doi.org/10.1002/ajmg.a.31092

Table 1. 3D facial anthropometric measurements in subjects with ATS as compared to healthy subjects: linear distances and ratios.

Measurement	Definition	Mean z-score	SD	P value
LINEAR DISTANCES				
Vertical distances				
tr-n	forehead height	-0.4	0.6	ns
n-pg	facial height	-1.3	0.6	<0.001
n-sn	upper facial height	-0.6	0.6	<0.01
sn-pg	lower facial height	-1.4	0.7	<0.001
os_r-or_r	right orbit height	-0.6	0.7	
os_l-or_l	left orbit height	-0.5	0.7	
sa_r-sba_r	right ear height	-0.2	0.7	ns
sa_l-sba_l	left ear height	-0.4	1.1	ns
sn-ls	nasolabial philtrum length	-1.5	0.9	<0.001
ls-sto	upper vermillion height	-0.5	1.2	ns
sto-li	lower vermillion height	0.1	0.6	ns
t_m-go_m	mandibular ramus length	-2.1	0.4	<0.001
Horizontal distances				
en_r-en_l	inner canthal width	0.6	0.7	ns
en_r-ex_r	right intercanthal width	-1.2	0.4	<0.001
en_l-ex_l	left intercanthal width	-1.6	0.6	<0.001
t_r-t_l	facial width	-0.8	0.8	<0.01
al_r-al_l	nose width	1.0	0.8	<0.01
pra_r-pa_r	right ear width	0.2	0.9	ns
pra_l-pa_l	left ear width			
cph-cph	nasolabial philtrum width	0.3	0.9	ns
ch_r-ch_l	mouth width	-0.6	1.5	ns
go_r-go_l	mandibular width	0.1	0.9	ns
Anteroposterior distances				
t_m-n	upper facial depth	-1.0	1.0	<0.01
t_m-sn	mid facial depth	-1.9	0.7	<0.001
t_m-pg	lower facial depth	-2.3	0.9	<0.001
snt_r-int_r	right nostril axis length	-1.8	0.9	<0.001
snt_l-int_l	left nostril axis length	-1.6	0.7	<0.001
pg-go_m	mandibular body length	-0.2	1.0	ns
RATIOS				
(t_m-go_m)/(sn-pg)	posterior/anterior facial height (FHI)	-1.2	0.5	<0.001
(t_r- t_l)/(n-pg)	facial width/ height	0.9	1.0	<0.01
(al-al)/(n-sn)	nasal width/ length ratio	1.4	0.5	<0.001

r = right, l = left, m = mid-landmark; FHI: facial height index.
P value: probability value of Student's t test (significance of the z-score value); ns: not significant ($p \geq 0.01$).

Table 2. 3D facial anthropometric measurements in subjects with ATS as compared to healthy subjects: angles.

Measurement	Definition	Mean z-score	SD	P value
ANGLES				
Angles in the frontal plane				
en_r-ex_r vs. TH	right palpebral fissure inclination	-0.9	0.6	<0.001
en_l-ex_l vs. TH	left palpebral fissure inclination	-0.8	0.4	<0.001
Angles in the sagittal plane				
n-sn-pg	facial convexity, except nose	0.4	1.2	ns
sn-n-prn	nasal convexity	0.1	0.7	ns
t_r-go_r-pg	right mandibular angle	0.9	1.3	ns
t_l-go_l-pg	left mandibular angle	0.9	1.7	ns
os_r-or_r vs. TH	inclination of right orbit	1.1	1.3	ns
os_l-or_l vs. TH	inclination of left orbit	0.8	1.2	ns
(t_m -n)-(go_m-pg)	facial divergence (midfacial to mandibular plane angle)	1.1	0.7	<0.001
Angles in the horizontal plane				
t_r-n-t_l	upper facial convexity	0.3	0.1	ns
t_r-prn-t_l	middle facial convexity	1.1	1.0	<0.01
t_r-pg-t_l	lower facial convexity	1.8	0.9	<0.001
al_r-prn-al_l	interalar angle	0.8	0.7	<0.01

r = right, l = left, m = mid-landmark; TH = true horizontal.
P value: probability value of Student's t test (significance of the z-score value); ns: not significant ($p \geq 0.01$).

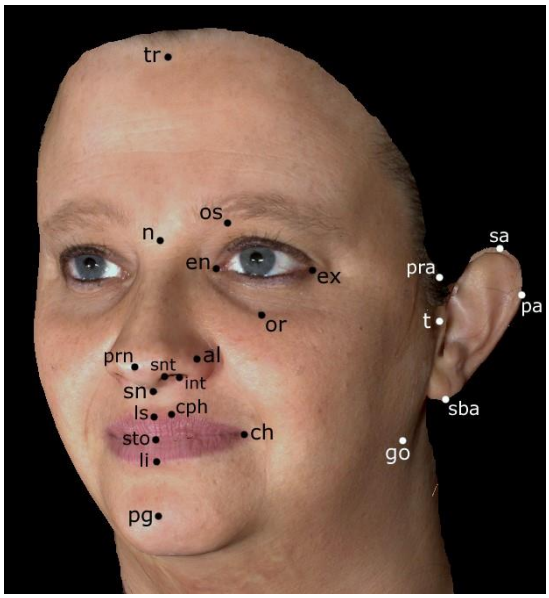

Figure 1. Soft-tissue landmarks used in the study, identified on the facial image of a 39-year-old female with ATS.

Midline landmarks: tr-trichion, n-nasion, prn-pronasale, sn-subnasale, ls-labiale superius, sto-stomion, li-labiale inferius, pg-pogonion. Paired landmarks: os-orbitale superius, en-endocanthion, ex-exocanthion, or-orbitale, al-alare, snt-superior point of the nostril axis, int-inferior point of the nostril axis, cph-crista philtri, ch-cheilion, t-tragion, go-gonion, pra-preaurale, sa-superaurale, pa-postaurale, sba-subaurale.

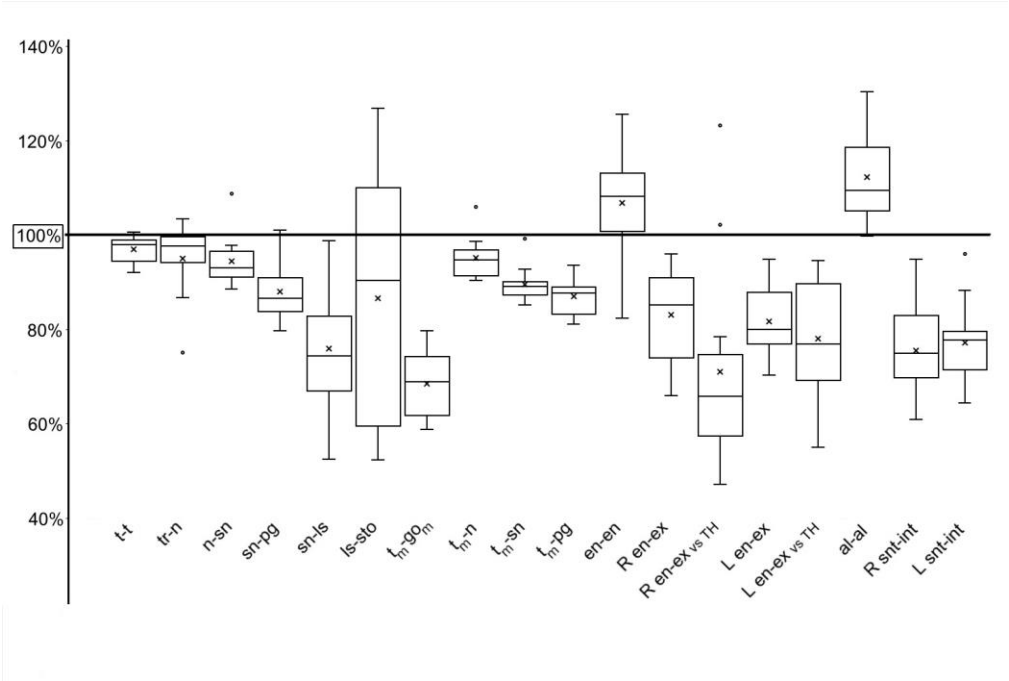

Figure 2. Box plot showing percentage variation of facial anthropometric parameters in ATS patients versus healthy subjects (mean value [x], median, 25% upper and lower quartile, minimum, maximum, and outliers).

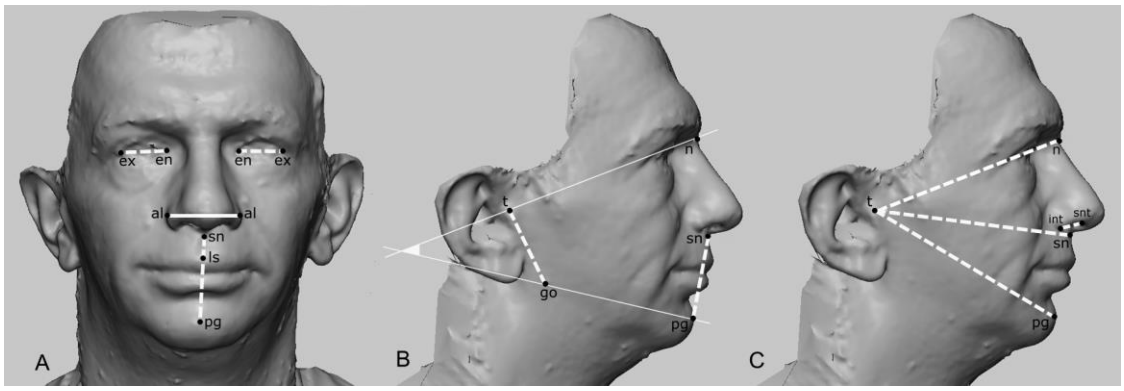

Figure 3. 3D facial image of a 49-year-old male with ATS. Anthropometric measurements with absolute z-score values ≥ 1 are highlighted.

Dotted lines: negative z-scores (decreased measurements); continue lines and angle: positive z-scores (increased measurements).

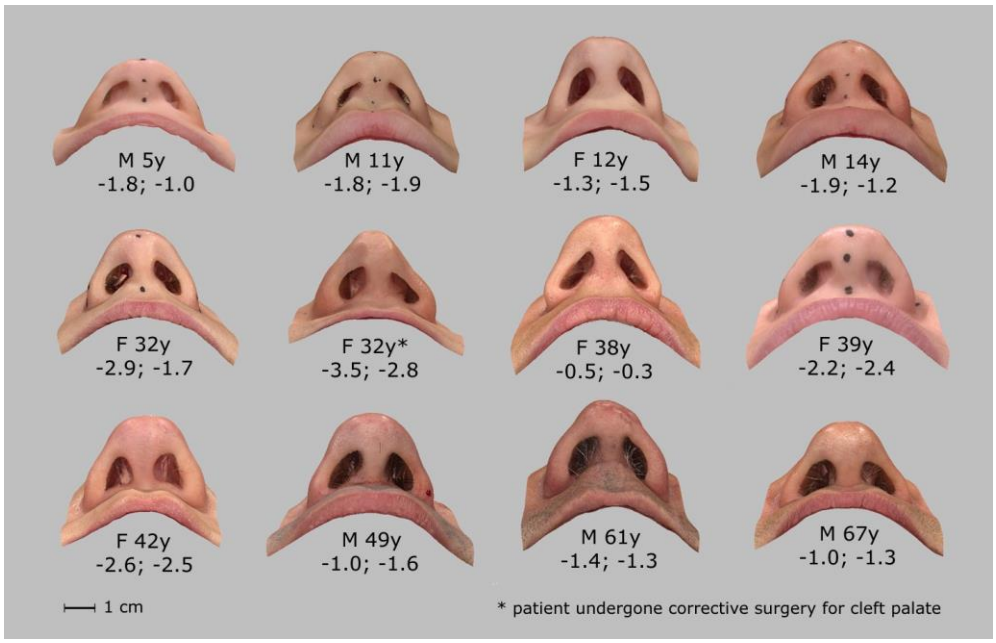

Figure 4. Worm's-eye view of nose base of patients with ATS. Sex (M-male, F-female, age (y-years), and individual z-score values for right and left nostril axis length are specified.